Journal of Cultural Heritage 73 (2025) 476–487

Contents lists available at ScienceDirect

Journal of Cultural Heritage

journal homepage: www.elsevier.com/locate/culher

Original article

Cobalt rich phases formed in processing natural erythrite at high temperatures

Lisa Bruzzone[a,*], Laura Gaggero[a], Judit Molera[b], Alessandro Zucchiatti[a,c]

[a] Department of Earth, Environment and Life Sciences, University of Genoa, Corso Europa 26, 16132 Genova, Italy
[b] MECAMAT, Facultat de Ciències, Tecnologia i Enginyeries, Universitat de Vic – Universitat Central de Catalunya, C. de la Laura, 13, 08500 Vic, BCN, Spain
[c] School of Physics, University of the Witwatersrand, 1 Jan Smuts av. Braamfontein 2000, Johannesburg, South Africa

ARTICLE INFO

Article history:
Received 29 August 2024
Accepted 8 April 2025

Keywords:
Cobalt dyes
Glaze
Erythrite
Synchrotron
Replicas of heritage processes

ABSTRACT

This study investigates whether natural erythrite was used before 1520 as a source of arsenic-free cobalt products for the production of blue glass and glazes. Historical records on glass and ceramics suggest a shift in cobalt sources or processing techniques around this time, with earlier European cobalt blue glass and glazes being arsenic-free and later ones containing significant arsenic levels. The aim is to determine the specific transformations of erythrite during firing, how it interacts with other compounds, and whether it forms phases that do not retain arsenic. To explore this, we conducted thermal treatments of erythrite alone and in combination with historically relevant minerals to assess its transformations and potential for arsenic removal. Materials characterization has been performed by XRPD, HT-SR-XRPD, XRF, and SEM-EDS.

The roasting of erythrite shows that the mineral decomposition begins at 227 °C, forming an amorphous phase with maximum arsenic loss by 635 °C. At 560 °C, cobalt arsenates (monoclinic and tetragonal $Co_3(AsO_4)_2$) crystallize, trapping arsenic within the structure. A transient cobalt arsenate appears at 627 °C but disappears at 755 °C, while at 775 °C, a cobalt-rich, arsenic-poor phase ($Co_{7.8}As_3O_{16}$) forms. Therefore, arsenic remains locked within stable cobalt arsenates, indicating that simple roasting of erythrite, as could have been achieved in 14th–16th century ovens, is insufficient to eliminate arsenic below detectable limits in medium-resolution techniques such as PIXE and XRF.

Further experiments following historical recipes using erythrite mixed with borax and calcite (as described by Isfahani) revealed the formation of an amorphous blue glass containing cobalt, arsenic, and boron, along with crystalline phases such as $NaCa_2Co_2(AsO_4)_3$, $Ca_3(AsO_4)_2$, as well as cobalt rich phases such as Co-borate ($Co_2Fe_{n.7}Ni_{n.3}BO_5$), with SiO_2 and Al_2O_3 spinels ($(Co,Ni,Fe,Al)_3O_4$.

1. Introduction

Cobalt chromogenic properties were known in Mesopotamia and Egypt at the beginning of the third millennium B.C.: it was used to give glass, enamels and powdered pigments a blue colour. It was exploited in the Mediterranean area, the continental Europe, the Near East and China. The glass industry in the Mediterranean area and the continental Europe, demanded cobalt, with continuity from the Egyptian epoch through the apex of the Roman Empire [1] and further on. The use of cobalt in ceramics is not as continuous as in the glass industry; it shows a hiatus between the 1st century B.C. and the end of 8th century A.D., when it reappears in the Abbasids faience of the city of Suse [2].

The wide geographical distribution and the long-time span of the use of cobalt, entails the exploitation of different mines as well as the evolution of the ores treatment to improve the dyes and pigments for the market. Significant examples of the diversity of products are the following.

The blue Egyptian glass of the 18th dynasty (1550–1292 B.C.), found in Amarna, contained cobalt extracted from the cobalt rich alums of the western oases of Kharga and Dakhla [3–5]. In the early Islamic Samarra faience (9th A.D.) cobalt is inferred to be extracted from Co, Ni, Fe mixed sulphide (mainly linnaeite), completely oxidised after high temperature roasting and melting [2]; linnaeite is inferred to originate in the Qamsar mine, where cobalt arsenate minerals also occur [6,7]. The production of Chinese

* Corresponding author.
E-mail address: lisa.bruzzone@edu.unige.it (L. Bruzzone).

https://doi.org/10.1016/j.culher.2025.04.007

blue and white porcelain employed, under several dynasties, either manganese rich local cobalt minerals (asbolane) or manganese poor minerals probably imported from Qamsar, the latter marked by the presence of arsenic [8].

Cobalt dyes and pigments used in and near Europe have been investigated, for example in French archaeological glasses [9,10] and ceramics from France, Italy, Spain, Maghreb, Uzbekistan, Syria and Egypt [11–17]. Both glasses and glazes, dated between the middle of the 15th century and the early 16th century, are characterized by the occurrence of Co and Ni. In these objects, very low As (below 100 ppm) has been detected by Instrumental Neutron Activation Analysis (INAA) [9,10] and was below detection limits in Particle-Induced X-ray Emission (PIXE) [12,13]. But the more recent pieces of the ensemble, dated from the beginning of 16th century onwards, are characterized by the presence of Co, Ni, Bi and As at high concentration (above 500 ppm and up to 0.7 % wt.).

The whole of data shows a relatively sudden change of raw materials in the transition between the 15th and 16th century A.D. The change is confirmed by the study of objects produced in the della Robbia workshop in Florence and accurately dated between 1445 and 1550, thanks to the reported chronicles of marriage celebrations, contracts of transports, tombs mounting, buildings construction and even by the date imprinted on the piece. The della Robbia ensemble has allowed establishing a sharp transition from an arsenic-free group of glazes to an arsenic-bearing one, around the year 1520 (-2, +1) [18].

The composition of blue glazes after 1520 is compatible with the geology of the Erzgebirge area where cobalt mostly occurs in the so called quartz-bearing five elements associations (Ag-Bi-Co-Ni-As) [19] with the absolute predominance of cobalt arsenides such as skutterudite ($CoAs_3$), clinosafflorite ($CoAs_2$), and the alteration product erythrite ($Co_3(AsO_4)_2{\cdot}8H_2O$) [20]. In addition, there is significant literature that attests a blue pigment request increase after 1520 [21] and that cobalt from the Erzgebirge was massively produced by roasting a selection of cobalt arsenides following the ancient process described by Johannes Kunckel [22].

The composition of blue glass and glazes from the middle of the 15th century and the early 16th century is essentially arsenic free but characterized (as well as the later production) by the presence of correlated Co and Ni, the transition to the later production being marked by the appearance of As, dispersed in the amorphous phase in Pb/Ca/As acicular crystals [23] and of lower amounts of Bi.

Two possible explanations have been proposed to account for the fast transition to As-bearing raw materials. (I) Dayton proposed that cobalt came as a by-product of smelting silver ore containing cobalt and heavier metals as impurities even at Micenean times [24,25]. (II) Soulier [9] supposed that before 1520 the cobalt was obtained by high temperature firing of erythrite ($Co_3(AsO_4)_2{\cdot}8H_2O$).

Indeed the coeval literature describes blue pigments long before 1520. In the “Fondaco dei Tedeschi” (the market place of the Germans) of Venice *caffaranum* is mentioned in 1328 [1]. Antonio da Pisa mentions *chafarone* in his 1395 treatise adding that it comes from Germany and it’s sold all over Europe [1]. Cennini in 1390–1437 describes a blue pigment as coming from *la Magna* (Germany) [26].

It is possible that a cobalt mineral without arsenic (e.g. sphaerocobaltite ($CoCO_3$), linnaeite ($(Co^{2+}Co^{3+})_2S_4$) and siegenite ($CoNi_2S_4$)) was used before 1520 to produce cobalt based products for the glass and pottery industry. However the documented wide diffusion of cobalt from Germany, the relevance of the mining district of the Erzgebirge in the German economy and the absolute predominance in the Erzgebirge area of Co-As minerals have been considered in an attempt to link both kinds of cobalt products (with and without arsenic) to the same cobalt minerals from the Erzgebirge; the distinction of the two being done by a different mineral treatment. This is the approach we took in our work.

In order to unravel the possible ore treatments, Molera et al. [27] focused on skutterudite ($CoAs_3$) as the primary cobalt mineral, demonstrating that roasting up to 900 °C, according to Kunckel’s description, stepwise transforms skutterudite into an arsenic-poor compound from $CoAs_3$ to $CoAs_2$ and finally to CoAs, but is not associated with arsenic loss to account for As absence occurring in pre-1520 glasses and glazes. Additionally, mixtures [27] intended to replicate those possible in the smelting of silver ore, as proposed by Dayton [24,25], and described by Agricola [28], failed to achieve an almost complete loss of arsenic. We have also to remark the substantial absence of silver in the 15th and 16th centuries blue glazes from the della Robbia [13] and other productions [10,11] of the same time. Silver is reported at ppm levels in much earlier productions like the Egyptian and Micenean one [24,29], the Pichvnari 5th B.C. one [30] and the 7th-8th century A.D. glass from Beirout [31].

With the same aim, Matin and Pollard [7] addressed cobalt ore from the historic mine of Kashan in present days Iran, particularly erythrite. They identified erythrite ($Co_3(AsO_4)_2{\cdot}8H_2O$), cobaltite (CoAsS) and asbolane ($((Co, Ni)_{1-y}(MnO_2)_{2-x}(OH)_{2-2x+2y}{\cdot}nH_2O$) as the three minerals that belong to the Kashan ore. Dispersing the ore in a water suspension, and selecting by sedimentation the lighter component, Matin and Pollard demonstrated that there is an enrichment in erythrite. Following the enrichment, they experimentally reproduced the processes reported in ancient literature from the area, roasting the mixtures up to 950 °C. Their results suggest that the Kashan processed cobalt ore is high in As and Fe, and lacks Ni, Cu or Zn. Noteworthy, dendrites of Co-As oxides and of Co-As-Fe sulphides were observed at the microscale.

2. Research aim

The goal of this work is to investigate whether natural erythrite was, before 1520, the source of arsenic free cobalt commercial products, used in the glass and ceramic industry to produce blue objects whose composition was consequently arsenic free. Thermal treatments of erythrite, both alone and in combination with other historically used minerals, were conducted. The study seeks to determine the specific transformations of erythrite during firing, to understand how it interacts with other compounds and whether it forms phases that do not retain arsenic.

3. Materials and methods

3.1. Materials

The natural cobalt ore from the Bou Azzer mine in Morocco occurs as mm to cm thick purple veins in dark grey host matrix (Fig. 1). Manual separation of erythrite (pink to purple crystals) from the thickest vein was followed by crushing and pulverisation in agate mortar. The replication of ancient mixtures was made by adding further components as detailed in paragraph 4.3.

3.2. Methods and analytical instruments

The ore sample was cut and embedded in resin to obtain a thin section for petrographic analysis by Transmitted Light Microscopy (TLM) and a metallographic polished thick section for subsequent Scanning Electron Microscopy (SEM).

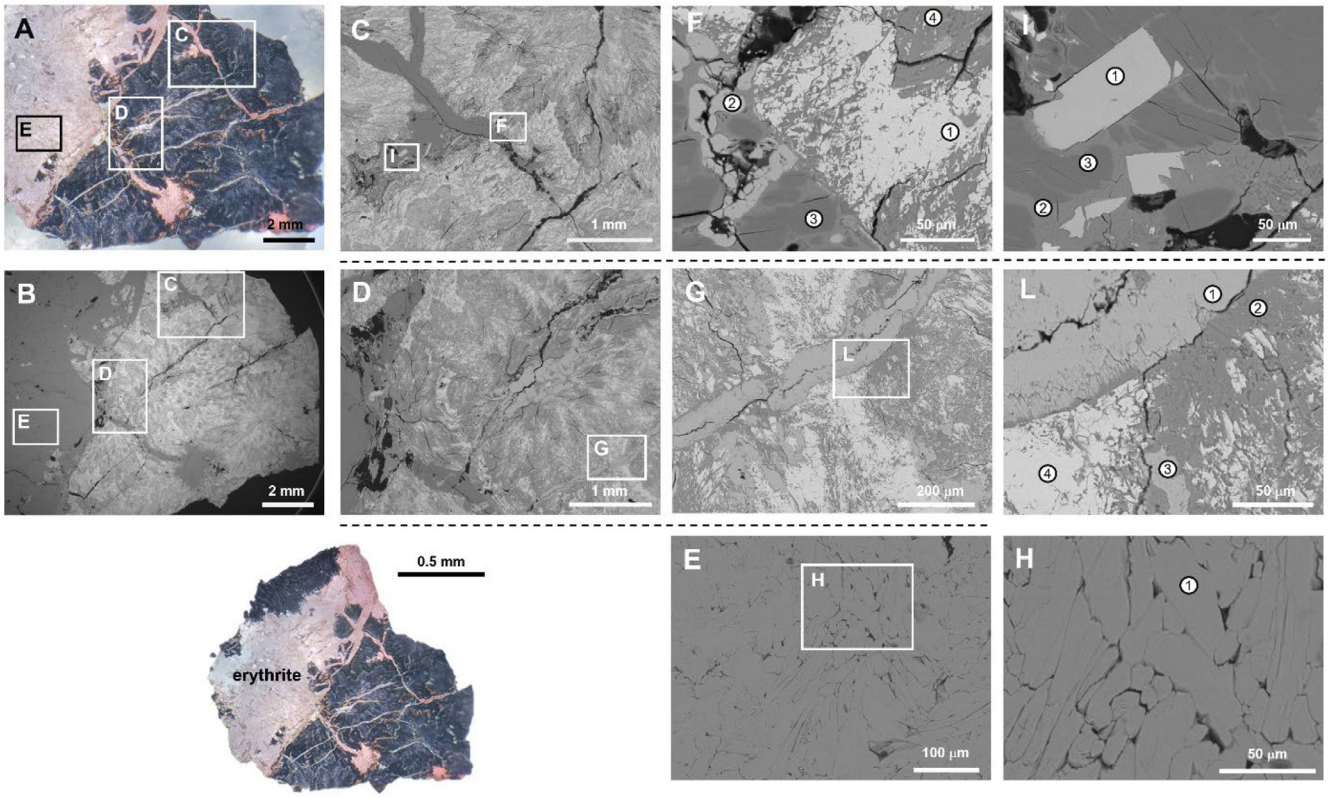

Fig. 1. Microphotographs of the ore from Bou Azzer. Starting from zone A (Reflected light OM) and B (SEM image) the subsequent enlargements (C, D, E, F, G, H, I, L) show SEM-EDS analysed spots (results in Table 1).

The ore and the mixtures were processed in two ovens sited at: I) the Department of Chemistry and Industrial Chemistry (DCCI) of the University of Genoa and II) the Universitat de Vic- Universitat Central de Catalunya (UVIC-UCC). The first is a TERSID tubular oven, provided with an internal quartz pipe for arsenic fumes escape. The samples were placed in alumina vessels for stepwise heating up to 900 °C. The second is a forced ventilation HOBERSAL oven provided of a ceramic stage for stepwise heating up to 900 and 1020 °C. The cooling ramp was controlled by an aspiration hood.

The characterization of natural and processed samples was done by SEM, also associated with Energy Dispersive Spectrometry (SEM-EDS), X-Ray Powder Diffraction spectrometry (XRPD) and X-Ray Fluorescence (XRF).

The Scanning Electron Microscope model Vega3 TESCAN at the DISTAV (Department of Earth, Environment and Life Sciences) of the University of Genoa was operated at 20.0 kV and a working distance of 15.0 mm. Compositional analysis was obtained by Energy Dispersion Spectrometry via the EDAX Apollo SDD detector. Analysis of spectra was performed by the eZAF method through the TEAM (Texture and Elemental Analytical Microscopy) EDS software. The Scanning Electron Microscope model Zeiss GEMINI (Shottky FE) at the Universitat Politècnica de Catalunya (UPC), was used in similar conditions (20.0 kV and a working distance of 7.0 mm).

Natural and processed samples were analysed with the following XRPD diffractometers: a) Rigaku Miniflex equipped with a HPAD (HyPix-400 MF 2D) hybrid pixel array detector and a 600 W X-ray source at the DCCI, University of Genoa operated at 40 kV between 5 and 90°, with a step of 0.02" b) Bruker ENDEAVOUR diffractometer operated at 38.28 kV from 5° to 90°, with a step of 2" at the DCCI, University of Genoa. Both instruments are equipped with a copper tube X-ray source (λ=1.5404 Å). Diffractograms are interpreted using the X'Pert HighScore Plus software.

High Temperature powder diffraction analyses in real time were performed at Materials Science and Powder Diffraction beamline (BL04-MSPD) at ALBA Synchrotron with the collaboration of their staff [32]. Erythrite and mixtures were ground in an agate mortar down to a final grain size below 80 µm before inserting them into a 500 µm diameter quartz capillary for the high-temperature synchrotron powder X-ray diffraction experiment (HT-SR-XRPD). The measurements were performed in transmission mode while rotating the capillary to improve particle statistics at an energy of 30 keV (wavelength $\lambda = 0.4133$ Å determined from a Si640d NIST standard). Diffraction data were collected by a 6-module Mythen detector covering an angular range of 60°(2θ) with a step size of 0.006°. A FMB Oxford hot air blower was used to heat from room temperature (RT) to 400 °C at 20 °C/min, from 400 °C to 900 °C at 10 °C/min, kept at maximum temperature for about 1 hour, in the case of erythrite, and for 5 min, in the case of mixtures, then cooled down from 900 °C to RT at 20 °C/min. The blower temperature was calibrated from the Si640d NIST cell parameter refined from diffraction data collected at the same conditions as the samples. During the heating and cooling stages data collection was performed sequentially with an acquisition time of 10 s.

After firing, additional scans were taken along the capillary to obtain XRD patterns of the mixtures fired at different temperatures. This is because the blower is in the central part, causing the rest of the capillary to experience lower temperatures until reaching a section where the sample is not heated. These scans are valuable because they lack the displacement typical of scans taken during heating, making them particularly useful for interpreting the new phases formed during the heating process.

The evolution of relative amounts of As and Co during step firing (see paragraph 4.2.2) was inspected by collecting XRF spec-

Table 1
Composition (expressed in % weight element) of the materials analysed in the areas and spots shown in Fig. 1. The possible corresponding compound is also indicated. In the Vivianite Group site M1 and M2= Mg, Fe, Co, Ni, (Mn, Cu, Zn), while site *X*=As, (P). In the Oxide site *A*=As, Fe, Co, Ni. In the Lollingite Group *A*=Fe, Co, Ni and *X*=As, S, (Sb). In the Skutterudite Subgroup *A*=Fe, Co, Ni *X*=As, (Sb). In the Cobaltite Group *A*=Co, Ni, Fe, *M*=As, (Sb, Bi) and *X* = *S*, (Se). In the Tsumcorite Group *A*= Ca, (Pb) *M*=Fe, Co, Ni, (Mn, Zn, Cu) and *X*=As, (P, V). b.d.l.= below detection limit.

Phase	Erythrite					Arsenolite			Clinosafflorite-Skutterudite		Cobaltite	Fe-Co-Lotharmeyerite
General formula	$M1M2_2(XO_4)_2 \cdot 8H_2O$ (Vivianite Group)					A_2O_3 Oxides			AX_2-AX_3 (Löllingite Group)-(Skutterudite Subgroup)		AMX (Cobaltite Group)	$AM_2(XO_4)_2(OH,H_2O)_2$ (Tsumcorite Group)
Zone (Fig. 1)	F	F	I	I	H	L	L	F	L	F	I	L
Spot	3	4	2	3	1	1	3	2	4	1	1	2
Element %												
Mg	b.d.l.	b.d.l.	b.d.l.	b.d.l.	0.8	–	–	–	–	–	–	–
Ca	–	0.3	0.2	–	–	–	–	–	–	–	–	11.9
Fe	0.8	3.1	1.8	0.9	1.4	0.4	0.3	0.2	2.4	1.9	0.6	22.6
Co	19.6	20.4	19.0	18.8	18.6	0.4	0.7	0.7	20.6	20.7	28.4	2.0
Ni	2.5	3.0	2.5	2.2	2.2	0.1	0.1	0.1	0.3	0.6	0.8	b.d.l.
As	30.1	40.6	35.7	26.9	25.1	74.9	74.7	74.8	74.7	75.4	50.4	37.7
S	–	0.6	0.3	–	–	–	–	–	2.0	1.3	19.8	0.3
O	15.9	21.6	18.4	14.6	14.7	24.2	24.2	24.2	–	–	–	24.5
Total	68.9	89.7	78.0	63.4	62.9	100	100	100	100	100	100	99.0
(Fe+Co+Ni)/As	0.96	0.84	0.83	1.04	1.13	0.01	0.02	0.02	0.40	0.39	0.75	0.87

tra from the Bruker Elio portable X-ray spectrometer at the DCCI, equipped with rhodium anode and operated at 30 kV. Incident beam diameter was 1 mm, and the X-ray spectra were collected by the 17 mm² Silicon Drift Detector (SDD) with a CUBE (Bruker) preamplifier that allows energy resolution < 140 eV for Mn Kα and better peak/background value.

4. Results

4.1. Characterization of the natural ore

4.1.1. Textural and EDS compositional features

The crosscutting veins of the Bou Azzer sample were investigated systematically by SEM-EDS microanalysis.

Quantitative analyses of the examined spots, indicated by numbers in Fig. 1 and reported in Table 1, highlighted the presence of different mineralogical phases.

The host rock consists of several minerals. The primary mineralisation is composed by a grey, opaque mineral (spot 4, zone L and spot 1 zone F), which exhibits a (Fe+Co+Ni)/As atomic ratio close to 0.4, intermediate between that of skutterudite ($CoAs_3$) and clinosafflorite ($CoAs_2$). White mineral veins at spots 1 and 3 in zone L and spot 2 in zone F have a composition compatible with that of arsenolite (As_2O_3). Idiomorphic prismatic crystals (spot 1 zone I) have been identified as cobaltite (CoAsS). In spot 2 zone L, the accessory mineral was identified, based on the (Fe+Co+Ni)/As ratio, as Fe-Co-lotharmeyerite.

The pink veins, that provided materials for the experiments described in the subsequent paragraphs, are mainly erythrite ($Co_3(AsO_4)_2 \cdot 8H_2O$) as suggested by the higher Co/As atomic ratio, despite minor Fe and Ni substitution in the mineral. It appears as a polyphase aggregate consisting of a massive (spots 3, 4 zone F and spots 2, 3 zone I) and a fibrous mineral (spot 1 zone H).

4.1.2. X-ray powder diffraction

The SR-XRPD results indicate that the hand-picked pink to purple crystals from the vein are mainly erythrite ($Co_{2.01}Fe_{0.74}Ni_{0.25}(AsO_4)_2 \cdot 8H_2O$, International Centre for Diffraction Data ICDD-code 01–086–0684) with minor content of clinosafflorite $CoAs_2$ and arsenolite As_2O_3 (Fig. 2A, RT pattern; Fig. 1 supplementary materials).

4.2. Thermal treatment of erythrite ore

4.2.1. Continuous stepwise heating under synchrotron radiation

To assess the erythrite phase stability under continuous heating, an experimental run was carried out at the ALBA synchrotron facility in Cerdanyola del Vallés (Barcelona) up to 900 °C. The starting material was mainly erythrite with minor arsenolite and clinosafflorite (Fig. 2A, RT pattern). At 227 °C erythrite began to decompose and at 285 °C only clinosafflorite and skutterudite were present. Possibly, skutterudite occurred in the starting material, but its peaks partially overlap those of erythrite and prevented identification. From 227 °C to 635 °C an amorphous phase was formed characterised by a very large background with two maximum peaks at d-spacing 4.13 Å ad 2.66 Å. At 560 °C, the monoclinic $Co_3(AsO_4)_2$ (ICDD code 01–073–1093) and the tetragonal $Co_3(AsO_4)_2$ (ICDD code 01–074–1930) cobalt arsenates began to form and fully developed at 620 °C; they remained stable during the heating and cooling process. At 627 °C another cobalt arsenate $Co_3(AsO_4)_2$ was formed but was unstable and disappeared at 755 °C (Fig. 2A and B). Peaks of this phase have been attributed to $Co_3(AsO_4)_2$ since, in the lack of a specific database they fit with a monoclinic structure like $Zn_{2.28}Mg_{0.72}(AsO_4)_2$ (ICDD 01–085–0317). At 775 °C a rhombohedral cobalt arsenate rich in cobalt and poorer in As is formed ($Co_{7.8}As_3O_{16}$, ICDD 01–070–1528). The monoclinic and tetragonal $Co_3(AsO_4)_2$ and $Co_{7.8}As_3O_{16}$ (ICDD codes 01–073–1093, 01–071–1930 and 01–070–1528) were stable also after the cooling cycle (Fig. 2A and B).

4.2.2. Step heating of erythrite powder

This experiment was designed for longer heating durations compared to the synchrotron experiment. A quantity of 0.0834 g of erythrite powder (ER) was thermally treated in the TERSID tubular oven (in an alumina crucible), according to the steps detailed in Table 2. Selected heating steps were inspected by XRPD and XRF.

The highest weight loss was observed after heating at 250 °C (Table 2) while a total weight loss of 25.1 % was recorded at the end of heating process.

The mineral and bulk composition of the untreated powder and that resulting after heating at 450, 650 and 900 °C (7 h) was characterised by both XRPD (Bruker D4 ENDEAVOR) and XRF. Considering the different performance of the D4-ENDEAVOUR diffractometer, compared to that of the MSPD, the diffractograms obtained

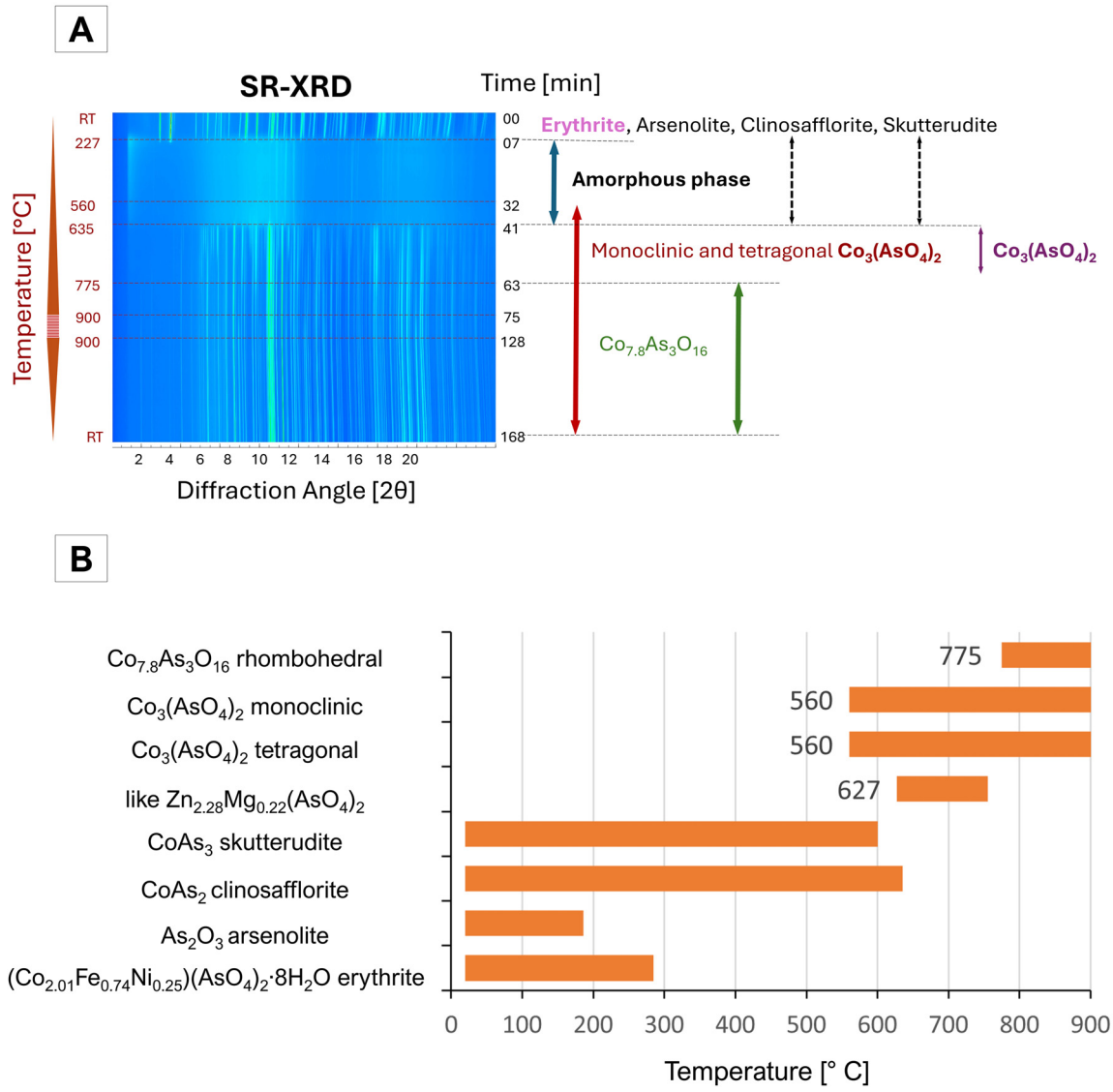

Fig. 2. A: Erythrite structural changes during heating from room temperature (RT) to 900 °C (HT-SR-XRPD). The marked temperatures correspond to the transitions reported in the text. B: Thermal stability range of cobalt crystalline phases during heating.

in this mineral processing confirm the results given by the synchrotron: i.e. the relevant transformation of the ER mineral structure – particularly the presence of a high background at 450 °C, due to a large amorphous content of the powder– but at the same time a limited arsenic loss on average because $Co_3(AsO_4)_2$ is formed at higher temperatures.

The moderate arsenic loss is also observed in the XRF spectra collected at various steps of the heating. In a fluorescence spectrum, the area of elemental characteristic peaks is proportional to the number of atoms of the element in the sample. If we normalize the ratios to the same Co peak areas, the change in the ratio will correspond to the relative change of the As quantity. The plot in Fig. 2 supplementary materials, proves that in the thermal process of Table 2 (four steps) that led to 900 °C, the As quantity did reduce progressively and ended at around 20 % bulk total loss, not distant from the loss observed while weighing the powder after each step and at the end of the cycle.

4.2.3. Heating of the erythrite fragment

Investigation of possible cobalt rich phases produced after heating was also done on the ER pink-purple fragment roasted in the TERSID tubular oven according to the steps indicated in Table 2, maintaining the maximum temperature of 900 °C for 14 h. In this case the maximum weight loss was experienced after the long roasting at 900 °C, while a total weight loss of 41 % was measured at the end of the cycle.

After all firings, the erythrite fragment was embedded in resin and polished for SEM-EDS analyses performed with the Zeiss GEMINI (Shottky FE) scanning electron microscope at the Universitat Politècnica de Catalunya. Table 1 supplementary materials reports the elemental concentrations for each point or area marked in Fig. 3 and the elemental ratios of interest to this study.

Even considering that the points measured before and after heating are not the same, the SEM results on the ER fragment, prove that new tabular crystals rich in Co and As are formed after heating at 900 °C for 14 h which correspond to $Co_3(AsO_4)_2$ detected by XRD. Moreover, the cobalt content increases with respect to arsenic in the fired fragment. The average value of the atomic ratio Co/As ranges from 0.79 in the natural ore (the parts roughly identified with erythrite; see Table 1) to 3.02 after roasting for 14 h and from an average value of the atomic ratio (Fe+Co+Ni)/As of 0.96 in the natural ore to 3.57 after roasting.

Table 2
Erythrite (powder and fragment) weight loss during step heating, RT= room temperature. *XRPD analyses were performed by the Bruker ENDEAVOUR diffractometer.

Action	Initial temperature [°C]	Final temperature [°C]	Gradient [°C]/ [min]	Time at constant temperature [min]	Initial weight [g]	Final weight [g]	Weight loss [%]
Erythrite powder							
Heating up to 250 °C	RT	250	3	–	0.0834	–	–
Roasting at 250 °C	250		constant	145	–	–	–
Return to RT	250	RT	no-control	–	–	0.0673	23.9
Heating up to 450 °C	RT	450	7	–	0.0673	–	–
Roasting at 450 °C	450		constant	145	–	–	–
Return to RT	450	RT	no-control	–	–	0.0653	3.1
Sampling for XRPD, XRF					0.0653	0.0577	
Heating up to 650 °C	RT	650	10	–	0.0577	–	–
Roasting at 650 °C	650		constant	180	–	–	–
Return to RT	650	RT	no-control	–	–	0.0567	0.2
Sampling for XRPD, XRF					0.0567	0.0533	–
Heating up to 900 °C	RT	900	15	–	0.0533	–	–
Roasting at 900 °C	900		constant	150	–	–	–
Return to RT	900	RT	no-control	–	–	0.0527	1.1
Sampling for XRPD, XRF							
Erythrite fragment							
Heating up to 200 °C	RT	200	2	–	0.0509	–	–
Roasting at 200 °C	200		constant	60	–	–	–
Return to RT	200	RT	no-control	–	–	0.0492	3.4
Heating up to 400 °C	RT	400	4	–	0.0492	–	–
Roasting at 400 °C	400		constant	60	–	–	–
Return to RT	400	RT	no-control	–	–	0.0416	18.3
Heating up to 900 °C	RT	900	9	–	0.0416	–	–
Roasting at 900 °C	900		constant	840	–	–	–
Return to RT	900	RT	no-control	–	–	0.0323	28.8
XRPD, SEM, EDS characterisations							

Is this sufficient to explain why in PIXE analysis of dated della Robbia sculptures, produced before 1520, arsenic was below detection limits [12,13]? On around 60 sculptures studied and almost 300 analyses on blue glaze points, PIXE did not detect arsenic in 120 of them. In case of arsenic absence, the PIXE spectra, deconvoluted by the Gupix analysis software [33], gave the values of Co concentrations in % weight, the arsenic minimum detection limit (As MDL) in ppm and the ratios of the two quantities, which are reported in Table 2 supplementary materials.

The As MDL distribution (Fig. 3A supplementary materials) has its maximum around 750 ppm with an average of 1061 ppm, while the distribution of Co/As MDL (Fig. 3B supplementary materials) is quite extended, with its peak around 5, an average of 8.29 and a few very high outliers.

Reasonably considering the data of Table 1 supplementary materials as representative of the average composition of roasted erythrite, Co results at an average of 46.56 % weight and As at an average of 21.66 % weight. Therefore reducing e.g. cobalt to 0.654 % weight (Table 1 supplementary materials) would bring As down to 0.30 % weight (3000 ppm), exceeding the average MDL found in the della Robbia pieces, i.e. 1061 ppm. Arsenic, although reduced by the selection of erythrite, maybe by precipitation [34] and further reduced by roasting should have been detected in the PIXE analysis.

4.3. Ore treatment according to ancient recipes

Several accounts of ore processing, not limited to the ore roasting, have been reported in ancient literature or have been passed on, by tradition, until documented in recent times. Some have been reproduced using skutterudite by Molera and coauthors [27].

To explore further recipes with erythrite, we reproduced the recipe given by Isfahani [35], first replicated by Matin and Pollard [34]. The mixture consists of 10 parts of ore powder, 5 parts of "*bureh-i-Yazd*" (ulexite or borax according to literature) and 5 parts of "*Tangar*" (identified as borax). Ulexite has formula $NaCaB_5O_9{\cdot}8H_2O$. In the lack of ulexite, the mixture "*bureh-i-Yazd*" and "*Tangar*" was replaced by borax ($Na_2B_4O_7{\cdot}10(H_2O)$) and calcite + calcium oxide obtaining a mixture identified as EM, composed of powdered erythrite ore (0.4002 g), of borax (0.3092 g) and of calcite + calcium oxide (0.0908 g). The mixture has been heated in the TERSID tubular oven at the University of Genoa inside an alumina crucible. The temperature was increased for 30 min up to 250 °C and maintained for an hour, then it raised in one hour up to 900 °C and remained at this value for 7 h. After that, the oven was switched off and left cool down to room temperature. The result was a solid body intermixed with the alumina crucible (that showed partly a blue colour). As much as possible of the produced body was recovered by breaking the crucible: part was ground for XRPD analysis and part was embedded in resin and polished for observation under polarized light and polished for SEM analysis.

The EM mixture (made with the same proportions detailed above) was heated up to 1020 °C in the HOBERSAL oven, over a kaolinitic crucible. The maximum temperature was reached after 10 h and was maintained for 30 min, then the oven was switched off. The heated mixture was characterised by SEM-EDS.

Other recipes for preparing cobalt pigments and dyes have been reported in literature by Olmer [36], Rochechouart [37], Schindler [38], Krieg [39]. All of them use borax as the main flux [7,34]. As regard erythrite the present work was limited to the Isfahani recipe. We have reproduced those of Schindler and Krieg [38,39] but only with clinosafflorite [40] which falls beyond the scope of this paper, focused on erythrite.

4.3.1. XRPD analysis of the EM mixture heated at 900 °C and 1020 °C

The reaction of erythrite with borax and calcite + calcium oxide after heating at 900 °C is evident in the diffractogram by HT-

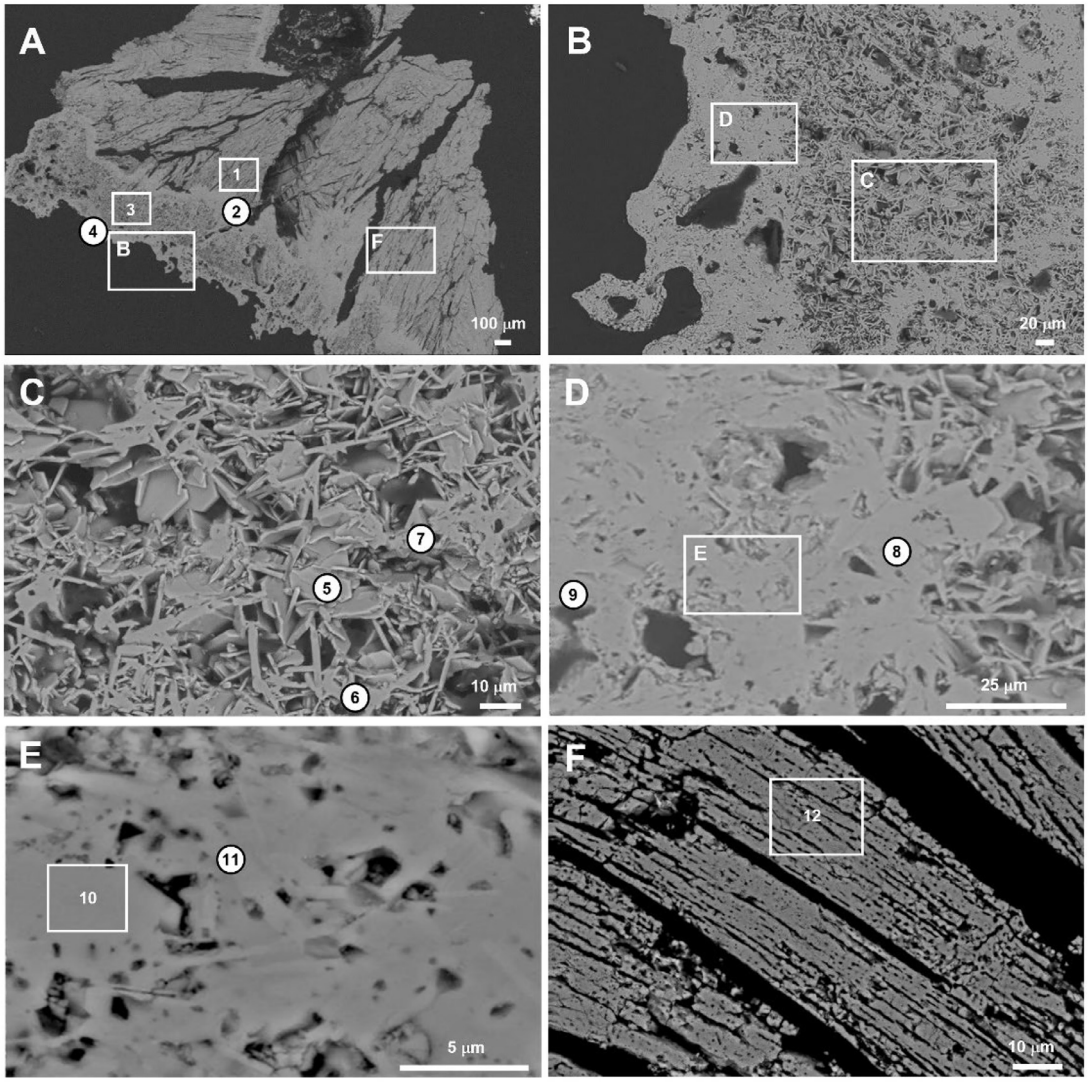

Fig. 3. SEM-BSE microphotographs of the roasted erythrite fragment (ER) zones. Boxes indicate addressed areas for spot analyses (results in Table 1 supplementary materials).

SR-XRPD synchrotron experiment. Three main phases (Fig. 4) are identified: 1) a Na- Ca- and Co- arsenate ($NaCa_2Co_2(AsO_4)_3$), 2) Ca-arsenate ($Ca_3(AsO_4)_2$) and 3) Co- borate (Co_3BO_5). Notably, a high background is due to the presence of a vitreous matrix.

At 1020 °C the mixture was fired inside a kaolinitic crucible. The reaction with SiO_2 and Al_2O_3 from the crucible gives a silica blue glass, and calcium sodium aluminosilicates are formed besides Na-, Ca- and Co- arsenates. It is not possible to identify Co-ludwigite or Co, Ni spinels in the XRD pattern.

4.3.2. Microscopic and compositional features of EM mixture heated at 900 °C and 1200 °C

After heating at 900 °C for 7 h, correlative images (Fig. 5A and B) under TLM show a blue dark matrix, pink euhedral crystals and radial acicular dark crystals. The SEM analysis was performed with the GEMINI (Shottky FE) scanning electron microscope at the Universitat Politècnica de Catalunya (Fig. 5C to 5H).

The composition of the material was measured by EDS on 17 spots, some corresponding to a point, some to a scanned area (Fig. 5 and Table 3). Analysis of the bright crystals at SEM (pink crystals in TLM) confirms that they correspond to $NaCa_2Co_2(AsO_4)_3$ (Fig. 5 spots 2, 3, 8, 13 and 14) previously identified by HT-SR-XRPD. The acicular crystals and amorphous phase contain boron (Fig. 5 spots 6, 9, 10 and 11) and are borates rich in Co, Fe and Ni. They correspond to the Co-ludwigite orthorhombic phase previously identified by HT-SR-XRPD. SEM-EDS analyses gives a composition of $Co_2Fe_{0.7}Ni_{0.3}BO_5$. The amorphous phase (Fig. 5 spots 5, 7, 16 and 17), dark blue under transmission optical microscopy and black under SEM-EDS, has the following element weight percentage composition: 9.79 % B, 45.71 % O, 10.01 % Na, 1.49 % Al, 0.47 % Si, 0.68 % S, 0.03 % K, 4.33 % Ca, 0.55 % Fe, 15.93 % Co, and 11.01 % As.

The results in Table 3 demonstrate that in the mixture the final Co/As atomic ratios can reach much higher values than in the erythrite alone, after heating at the same temperature, in correspondence with the acicular, hexagonal or rhombic section crystals identified in Fig. 5 (zone F, points 6 and 9; zone G, points 10, 11 and 12).

At 1020 °C, the mixture reacted with the silica and alumina of the kaolinitic crucible, and the final roasted mixture is completely blue (Fig. 6). The amorphous phase contains SiO_2 (53.0 wt. %), Al_2O_3 (20.9 wt. %), Na_2O (9.4 wt. %), CaO (4.4 wt. %), K_2O (1.4 wt. %), FeO (1.0 wt. %), NiO (0.6 wt. %), As_2O_3 (1.8 wt. %) and CoO (6.0 wt. %) (Fig. 6C area 2).

Boron was above detection limit (Fig. 7) in the amorphous phase but could not be quantified. At SEM the bright crystals cor-

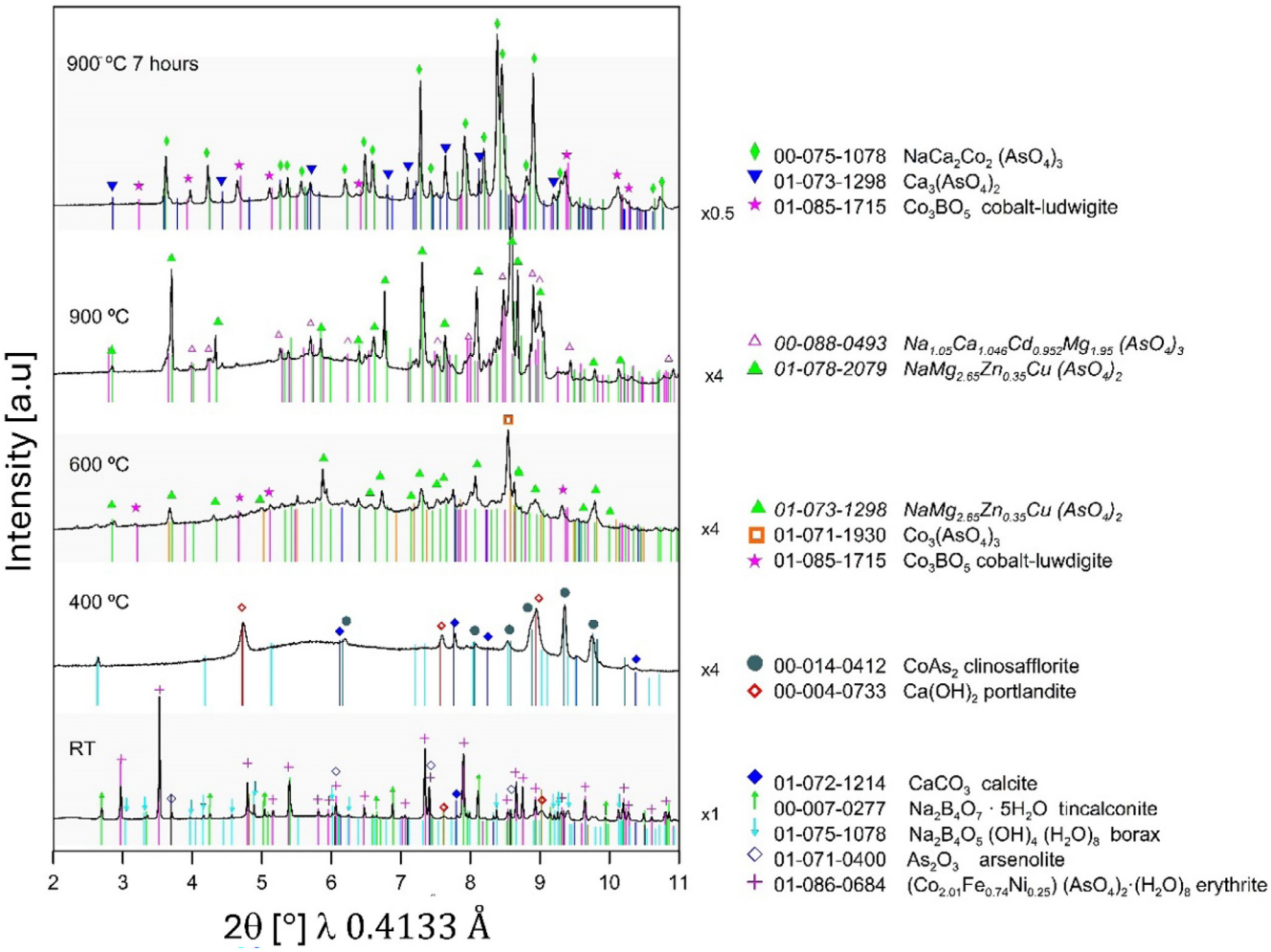

Fig. 4. SR-XRD patterns of the mixture EM before heating (RT) and during the thermal treatment at 400 °, 600 ° and 900 °C. The pattern at the top represents the mineral composition of the EM mixture heat-treated for 7 h at 900 °C inside the TERSID tubular oven. Symbols indicate the identified structures. Phases listed in italic correspond to virtual structures and not to real phases in the mixture, due to lack of Mg, Cu, Cd and Zn.

respond to $NaCa_2Co_2(AsO_4)_3$ (Fig. 6 spot 1), and other elongated bright crystals only contain Co, Fe and Ni (Fig. 6 spot 4). These crystals do not contain B and could possibly correspond to Fe, Ni, Co spinels which recall the pigment relics identified by Kleinmann [6] in Early Islamic blue glazes.

The transformation of Co_3BO_5 into Co_3O_4 takes place at temperatures above 150 °C [41]. Therefore, Co_3BO_5 could be converted in cobalt oxide (spinel, Co_3O_4). The Co/As atomic ratio increases further, again in correspondence with crystal structures embedded in the fused body (Fig. 6, zone C spectrum 4).

5. Discussion

Our investigation on possible thermal treatments that erythrite could have undertaken in the past, to obtain a cobalt secondary product to be used in the production of blue glass and ceramics has produced the following relevant evidence.

XRPD demonstrated that erythrite breaks down upon heating, forming an amorphous phase from 227 to 635 °C with the maximum weight and As loss. Then, at 560 °C, it begins to crystallize as different cobalt arsenates ($Co_3(AsO_4)_2$, monoclinic, tetragonal), and arsenic is retained in the new crystals and cannot be liberated from the fired powder or the fragment. At 627 °C an unstable cobalt arsenate is formed and disappears at 755 °C. Finally at 775 °C a poorer arsenic cobalt arsenate ($Co_{7.8}As_3O_{16}$) is formed. Therefore, three different cobalt arsenate phases remain at 900 °C retaining arsenic.

This explain why the simple roasting of erythrite up to 900 °C, as could be reached in 14th-16th century ovens, is not enough to remove the arsenic, neither completely, nor to such an extent to make it undetectable in medium resolution techniques, like PIXE and XRF. This is parallel to what has been found for skutterudite [27,42,43] and erythrite [34] in previous works. In the bulk, XRF analyses show a 22.4 % loss of arsenic with respect to Co. Similarly, SEM-EDS analysis on scattered points of a fragment of erythrite heated up to 900 °C gives an atomic ratio Co/As that goes from a minimum of 1.37 to a maximum of 6.19, not compatible e.g. with finding arsenic below detection limit in artistic 15th-16th century sculptures [12,13].

The most plausible hypothesis is that to obtain cobalt rich phases without arsenic from erythrite it is necessary to study the thermal treatment of a mixture of ingredients, prepared, as closely as possible, according to ancient recipes. In the present study we obtained new information on crystal and amorphous phases present after heating the erythrite mixed with borax and calcite, according to Isfahani [35]. With borax and calcite an amorphous blue glass is formed containing Co, As and B among others. Besides, $NaCa_2Co_2(AsO_4)_3$ and $Ca_3(AsO_4)_2$ we observed the formation of Co borate acicular crystals (Co-ludwigite), with a lower Fe and Ni content and much lower As. These acicular crystals, not

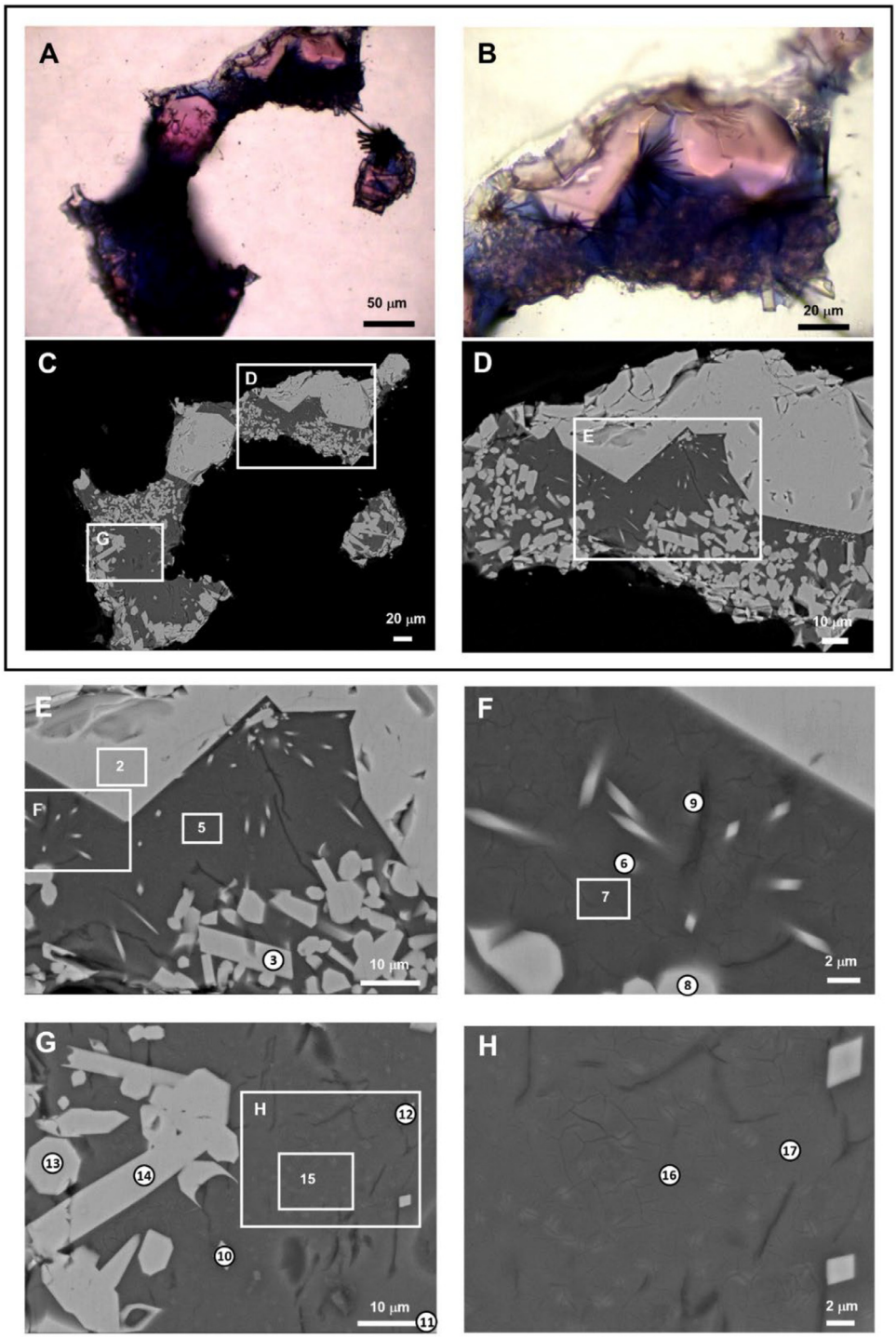

Fig. 5. Microphotographs of mixture EM after heating at 900 °C for 7 h. Zones A and C, and B and D show a comparison between transmitted light OM (TLM) and SEM,. E, F, G and H are enlargements showing the spots and areas analysed by SEM-EDS (results in Table 3).

observed before, have been identified by XRPD and SEM-EDS as $Co_2Fe_{0.7}Ni_{0.3}BO_5$.

Like the findings of Molera et al. [27] in their work on skutterudite, it has been observed that a blue amorphous phase containing cobalt is formed, including different arsenates of Ca, Na, and Co. Sodium from borax and calcium from calcite favour the formation of these arsenates. These results parallel what Molera et al. [27] found in skutterudite mixtures, where Pb and Ca promoted the formation of arsenate crystals $(Ca,Pb)_5(AsO_4)_3(F,Cl,OH)$, but in that case with a hedyphane structure. With borax and calcite, the structure of the arsenates is not hedyphane (hexagonal), but instead, $NaCa_2Co_2(AsO_4)_3$ and $Ca_3(AsO_4)_2$ are formed.

The amorphous blue glass contains also Co, As and B. Therefore, the roasting process of erythrite mixture would result in a blue glass that could have been crushed and ground to be sold as cobalt pigment. In any case, since arsenic does not completely disappear and remains trapped in the crystalline phases of sodium, calcium, cobalt arsenates, or even in cobalt arsenates, such treatments do not explain the low arsenic content in ceramics dating before A.D. 1520.

Table 3
The composition in % weight element of the materials analysed in the areas and spots shown in Figs. 5 and 6 for the EM mixture fired at 900 °C or at 1020 °C, b.d.l.=below detection limit. D.N.Q.= Detected but Not Quantified.

Zone	Spectrum (Point/Area)		% Weight elements														Atomic ratios	
			B	O	Na	Mg	Al	Si	S	K	Ca	Ti	Fe	Co	Ni	As	Total	Co/As	(Fe+Co+Ni)/As
Mixture EM 900 °C																			
E	2	A	b.d.l.	29.1	4.4	b.d.l.	b.d.l.	b.d.l.	b.d.l.	b.d.l.	13.9	b.d.l.	0.4	18.5	2.5	31.1	100	0.76	0.88
	3	P		28.4	4.2						13.8		0.7	18.8	2.4	31.7	100	0.75	0.88
	5	A		45.5	13.1		2.9	0.4	1.0		5.9		0.5	18.3	b.d.l.	12.4	100	1.88	1.93
F	6	P	b.d.l.	37.1	8.3	b.d.l.	2.2	0.3	0.5	b.d.l.	2.2	b.d.l.	7.9	30.3	3.5	7.7	100	5.02	6.99
	7	A		46.7	11.6		2.7	0.4	0.9		5.9		0.5	19.2	b.d.l.	12.0	100	2.04	2.10
	8	P		28.9	4.4		b.d.l.	b.d.l.	b.d.l.		13.7		0.8	18.6	2.2	31.5	100	0.75	0.87
	9	P		39.4	8.5		2.5	0.6	0.4		2.3		6.5	28.4	3.2	8.0	100	4.49	6.09
G	10	P	b.d.l.	29.2	b.d.l.	b.d.l.	1.2	b.d.l.	b.d.l.	b.d.l.	0.3	b.d.l.	14.7	45.1	7.3	2.2	100	26.16	39.46
	11	P		30.2			b.d.l.				b.d.l.		13.9	46.0	6.9	3.0	100	19.16	26.17
	12	P		30.4	2.7		1.0				0.6		12.8	42.7	6.0	3.8	100	14.33	20.90
	13	P		26.9	4.2		b.d.l.				14.6		0.7	19.7	2.1	31.7	100	0.79	0.91
	14	P		26.8	4.5			0.3			14.2		0.7	19.5	2.4	31.5	100	0.70	0.92
	15	A		45.4	13.5		2.2	0.6	0.8		6.0		0.7	18.5	b.d.l.	12.3	100	1.91	1.98
H	16	P	8.71	45.9	8.3	b.d.l.	1.9	1.5	0.9	b.d.l.	5.4	b.d.l.	0.7	16.6	b.d.l.	10.1	100	2.10	2.19
	17	P	b.d.l.	39.0	9.1		2.5	b.d.l.	1.3		8.9		1.1	26.1		12.0	100	2.77	2.89
Mixture EM 1020 °C																			
B	1	P	b.d.l.	34.7	3.9	1.0	0.3	1.11	b.d.l.	b.d.l.	12.5	b.d.l.	b.d.l.	14.3	1.4	30.7	100	0.59	0.65
C	2	P	b.d.l.	48.5	6.7	b.d.l.	10.4	24.25	b.d.l.	1.2	3.3	b.d.l.	0.6	4.0	b.d.l.	1.1	100	4.47	5.23
	3	P		39.3	1.1	1.5	4.7	9.13		b.d.l.	8.8		b.d.l.	27.2		8.2	100	4.22	4.22
	4	P		26.4	b.d.l.	b.d.l.	2.9	0.85			0.2	0.5	13.0	35.4	19.8	1.0	100	46.87	91.41
	5	A		39.5		1.9	2.4	9.06			4.0	b.d.l.	0.7	37.8	b.d.l.	4.5	100	10.58	10.79
D	6	P	b.d.l.	49.6	5.1	b.d.l.	13.4	24.98	b.d.l.	b.d.l.	5.9	b.d.l.	b.d.l.	0.8	b.d.l.	0.1	100	6.70	6.70
	7	P		47.5	4.1		7.6	17.32		0.7	7.1			12.3		3.2	100	4.85	4.85

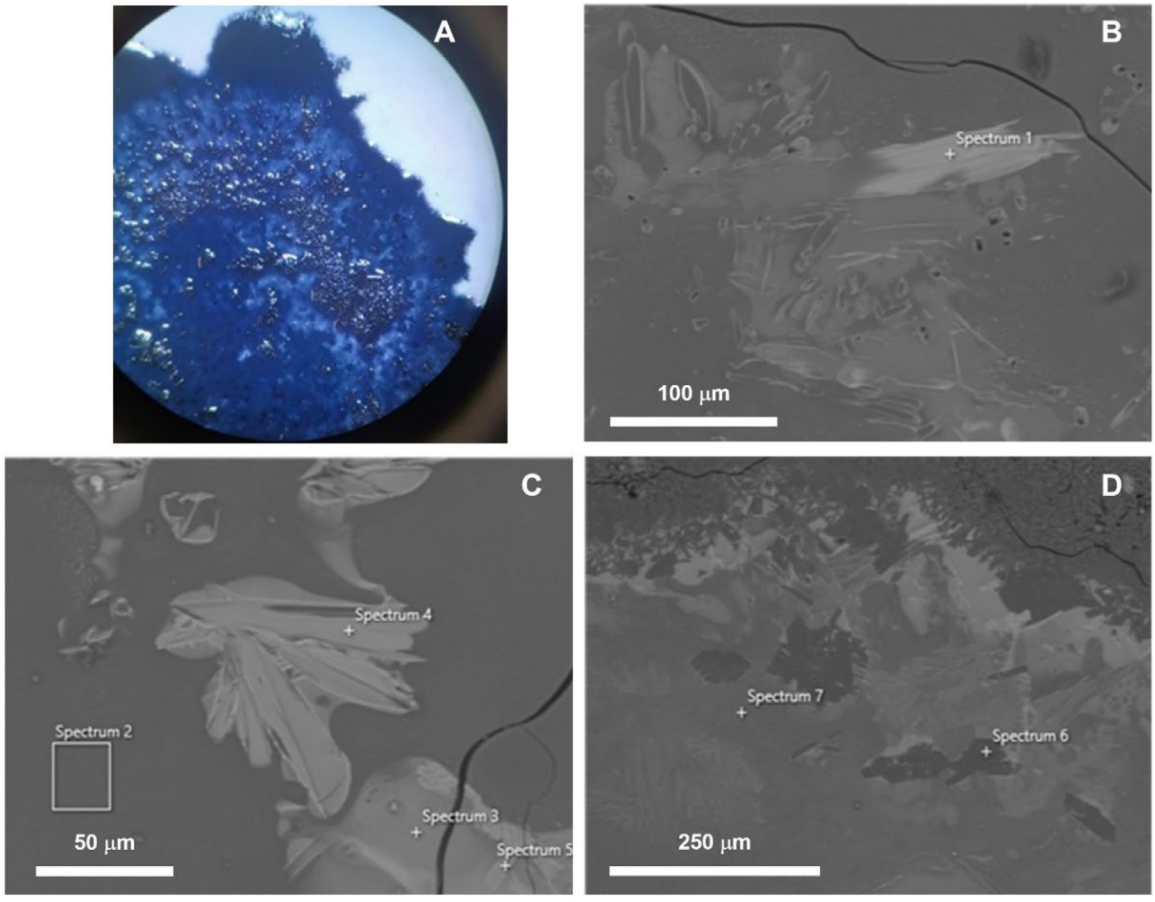

Fig. 6. Microphotographs of mixture EM after heating at 1020 °C. Zone A shows the mixture under the stereomicroscope. Zones B, C, D are SEM images with spots and areas analysed by SEM-EDS (results in Table 3). Scale bar in photos.

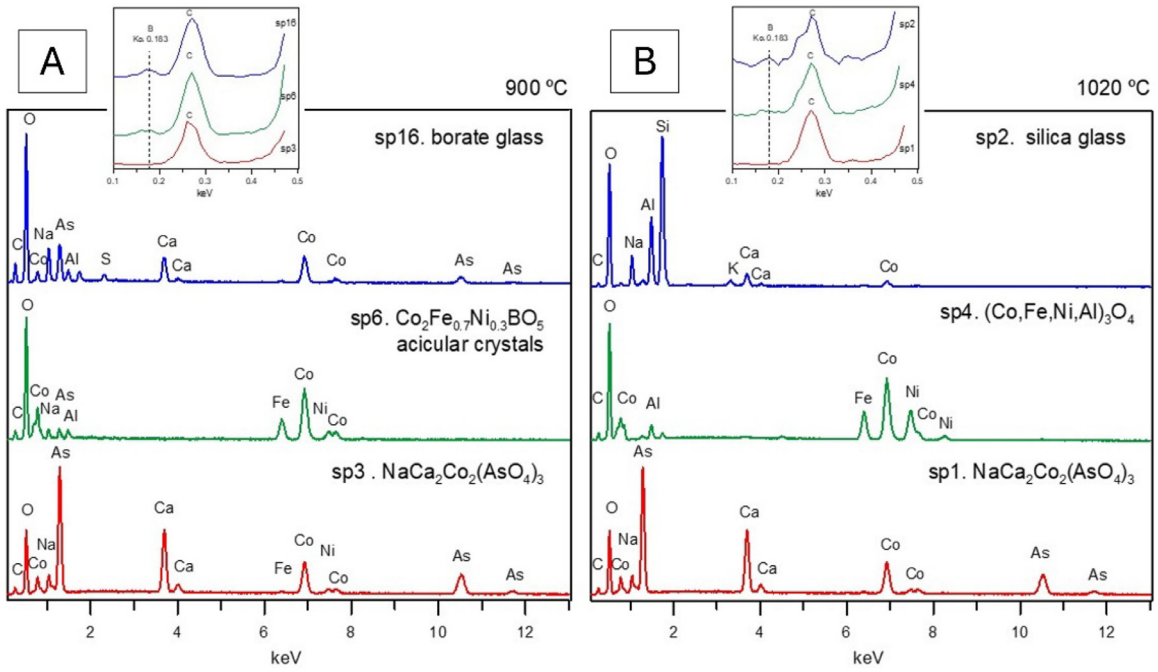

Fig. 7. SEM-EDS spectra of glass and crystalline phases in mixture EM heated at 900 °C (A) and at 1020 °C (B). On the upper part, the detail of the boron peak in all EDS spectra (compositions in Table 3).

6. Conclusions

In conclusion, this study has allowed for the identification of the crystalline phases that form during the firing of erythrite and the mixture of erythrite with borax and calcite, some of which retain arsenic ($Co_3(AsO_4)_2$, $Co_{7.8}As_3O_{16}$, $NaCa_2Co_2(AsO_4)_3$ and $Ca_3(AsO_4)_2$). Furthermore, it has been possible to precisely determine the composition and structure of the acicular "arsenic-free" crystalline phases. In this case, they correspond to borates rich in Co, Fe, and Ni with a Co-ludwigite structure ($Co_2Fe_{0.7}Ni_{0.3}BO_5$) and with SiO_2 and Al_2O_3 spinels $(Co,Ni.Fe,Al)_3O_4$. Therefore, the identification of acicular crystals rich in Co, Ni, and Fe will require further analysis of ancient ceramics to determine if they contain boron or not. The detection of boron is not easy because it is a light element, and its detection must be done under very high-resolution. However, it is an interesting result as it will help determine if boron was indeed used in pigment production.

In conclusion, since arsenic is uptaken in the crystalline phases of sodium, calcium, and cobalt arsenates, such treatments fail to explain the low arsenic content found in ceramics dating before A.D. 1520. However in the current work we have demonstrated that cobalt may form "arsenic-free" crystalline phases with iron and nickel.

CRediT authorship contribution statement

Lisa Bruzzone: Investigation; Experiment design; Data acquisition; Writing – review & editing. **Alessandro Zucchiatti:** Investigation; Experiment design; Methodology; Data acquisition; Conceptualization; Supervision; Writing – original draft. **Laura Gaggero:** Conceptualization; Supervision; Methodology; Writing – review & editing; Visualization; Funding. **Judit Molera:** Experiment design; Methodology; Data acquisition; Writing – review & editing.

Acknowledgments

This research was carried out with the support of the *Analisi delle proprietà microstrutturali, chimico-fisiche di materiali inorganici; determinazioni quantitative della composizione mineralogica di materiali naturali e delle proprietà tecniche dei materiali litici* Laboratory funds, DISTAV, University of Genoa and the support of Science and Technology for Earth and Environment doctoral funds (39° cycle) I.4.1 Borse PNRR Patrimonio Culturale CUP: D32B23002.

Judit Molera is grateful to the project PID2022–137783OB-I00 funded by the Ministerio de Ciencia e Innovación (Spain). The experiments were performed at BL04 MSPD Beamline at ALBA Synchrotron Facility with the collaboration of Alba Staff, project number 2023027361.

The authors warmly acknowledge Elena Castagnotto, Pietro Manfrinetti, Trinitat Pradell, Laura Negretti and Mustapha Haddad for their support at different phases of our work.

The authors are also grateful to the University Moulay Ismail of Meknes for providing us with the mineralogical sample from Bou Azzer.

Supplementary materials

Supplementary material associated with this article can be found, in the online version, at doi:10.1016/j.culher.2025.04.007.

References

[1] F. Delamare, Aux origines des bleus de cobalt: les débuts de la fabrication du saffre et du smalt en Europe occidentale, Comptes rendus des Séances de l'Académie des Inscriptions et Belles-Lettre 153e année (1) (2009) 297–315, doi:10.3406/crai.2009.92472.

[2] Y. Porter, Origines et diffusion du cobalt utilisé en céramiques à l'époque médiévale: ètude preliminaire, in: VI^{ème} Congrès International sur la céramique médiévale en méditerranée, Recuil des Pré-actes held in Palais des Congrès, Aix-en-Provence 13-18 November 1995, Narrations Ed, 1997, pp. 505–512. Aix.

[3] A. Kaczmarczyk, The sources of cobalt in ancient Egyptian pigments, in: J. Olin, M.J. Blackman (Eds.), Proceedings of the 24th international Archaeometry Symposium held in Washington 14-18 May 1984, Washington Smithsonian Institution Press, DC, 1986, pp. 369–376.

[4] A.J. Shortland, M.S. Tite, I. Ewart, Ancient exploitation and use of cobalt alums from the western oases of Egypt, Archaeometry. 48 (1) (2006) 153–168 Singapore, doi:10.1111/j.1475-4754.2006.00248.x.

[5] A.K. Hodgkinson, D.A. Frick, Identification of cobalt-coloured Egyptian glass objects by LA-ICP-MS: a case study from the 18th dynasty workshops at Amarna,

Egypt, Mediterranean Archaeol. Archaeom. 20 (1) (2020) 45–57, doi:10.5281/zenodo.3605660.
[6] B. Kleinmann, Cobalt-pigments in the early Islamic blue glazes and the reconstruction of the way of their manufacture, in: E. Pemicka, G. Wagner (Eds.), Proceedings of the 90th International Symposium on Archaeometry held in Heidelberg April 2-6, 1991, Birkhauser, Basel, 1991, pp. 327–336.
[7] M. Matin, M. Pollard, Historical accounts of cobalt ore processing from the Kashan Mine, Iran, Iran, J. Br. Inst. Persian Stud. (2015) 171–183, doi:10.1080/05786967.2015.11834755.
[8] R. Wen, C.S. Wang, Z.W. Mao, Y.Y. Huang, A.M. Pollard, The chemical composition of blue pigment on Chinese Blue-and-White porcelain of the Yuan and Ming dynasties (AD 1271-1644), Archaeometry. (49) (2007) 101–115, doi:10.1111/j.1475-4754.2007.00290.x.
[9] I. Soulier, B. Gratuze, J.N. Barrandon, D. Foy, The origin of cobalt blue pigments in French glass from the bronze age to the eighteen century, in: Archaeometry, Ankara, 1994, pp. 133–140.
[10] B. Gratuze, I. Soulier, J. Barrandon, D. Foy, De l'origine du cobalt dans les verres, Revue d'Archéometrie (16) (1992) 97–108, doi:10.3406/arsci.1992.895.
[11] B. Gratuze, I. Soulier, M. Blet, L. Vallauri, De l'origine du cobalt: du verre à la céramique, Revue d'Archèometrìe (20) (1996) 77–94, doi:10.3406/arsci.1996.939.
[12] A. Zucchiatti, A. Bouquillon, J. Castaing, J.R. Gaborit, Elemental analyses of a group of glazed terracotta angels from the Italian renaissance, as a tool for the reconstruction of a complex conservation history, Archaeometry 45 (3) (2003) 391–404, doi:10.1111/1475-4754.00116.
[13] A. Zucchiatti, A. Bouquillon, I. Katona, A. D'Alessandro, The 'della Robbia blue': a case study for the use of cobalt pigments in ceramics during the Italian renaissance, Archaeometry. 48 (1) (2006) 131–152, doi:10.1111/j.1475-4754.2006.00247.x.
[14] J. Pérez-Arantegui, M. Resano, E. García-Ruiz, F. Vanhaecke, C. Roldán, J. Ferrero, J. Coll, Characterization of cobalt pigments found in traditional Valencian ceramics by means of laser ablation-inductively coupled plasma mass spectrometry and portable X-ray fluorescence spectrometry, Talanta 74 (5) (2008) 1271–1280 Issue, doi:10.1016/j.talanta.2007.08.044.
[15] J. Molera, J. Coll, T. Pradell, The blue ceramic from Manises'Obradors quarter: technology of production. Tecnología de los vidriados en el oeste mediterráneo: tradiciones islámicas y cristianas, in: J. Coll Conesa, E. Salinas Pleguezuelo (Eds.), Catálogo De Publicaciones Del Ministerio De Cultura y Deporte, Gobierno de España, 2021, pp. 257–273. https://www.libreria.culturaydeporte.gob.es/libro/tecnologia-de-los-vidriados-en-el-oestemediterraneo-tradiciones-islamicas-y-cristianas_5354/.
[16] A. Zucchiatti, A. Azzou, M. El Amraoui, M. Haddad, L. Bejjit, S.Ait Lyazidi, Pixe Analysis of Moroccan architectural glazed ceramics of 14th-18th Centuries, Int. J. PIXE (2011) 175–187, doi:10.1142/S0129083509001862.
[17] J. Molera, J. Coll, T. Pradell, The blue ceramic from manises' obradors quarter: technology of production La cerámica azul del taller de obradors de manises: Tecnología De Producción Vidriados Medievales y Modernos En La Península Ibérica. Investigaciones Recientes, 257–273.
[18] G. Pappalardo, E. Costa, C. Marchetta, L. Pappalardo, F.P. Romano, A. Zucchiatti, P. Prati, P.A. Mandò, A. Migliori, L. Palombo, M.G. Vaccari, Non-destructive characterization of Della Robbia sculptures at the Bargello Museum in Florence by the combined use of PIXE and XRF portable systems, J. Cult. Herit. 5 (2004) 183–188, doi:10.1016/j.culher.2003.08.002.
[19] S.A. Kissing, Five elements (Ni-Co-As-Ag-Bi) veins, Geosci. Canada 19 (3) (1992) 113–124.
[20] T. Seifert, D. Sandmann, Mineralogy and geochemistry of indium-bearing polymetallic vein-type deposits: implications for host minerals from the Freiberg district, Eastern Erzgebirge, Germany, Ore Geol. Rev. 28 (2006) 1–31, doi:10.1016/j.oregeorev.2005.04.005.
[21] C. Meltzer, Bergklaufftige Beschreibung der Bergck-Stadt Schneeberg, Schneeberg, 1684.
[22] J. Kunckel, Ars Vitraria Experimentalis, Frankfurt and Liepzig, 1679.
[23] C. Viti, I. Borgia, B. Brunetti, A. Sgamellotti, M. Mellini, Microtexture and microchemistry of glaze and pigments in Italian Renaissance pottery from Gubbio and Deruta, J. Cult. Herit. 4 (2003) 199–210, doi:10.1016/S1296-2074(03)00046-3.
[24] J.E. Dayton, Egyptian blue or kyanos and the problem of cobalt, in: Minerals, Metals, Glazing and Man, Harrap London, 1978, pp. 451–462.
[25] J.E. Dayton, Geological evidence for the discovery of cobalt blue glass in mycenaean times as a by-product of silver smelting in the Schneeberg area of the bohemian Erzgebirge, in: Actes Du XX Symposium International D'archéométrie Held in Paris, March 26-29 1980). 'Revue d'Archéométrie: Bulletin de Liaison du Groupe des Méthodes Physiques Et Chimiques De L'archéologie, 3, 1980, pp. 57–61, doi:10.3406/arsci.1981.1131.
[26] *Re*-edited by C C. Cennini, Il libro dell'arte" 1390-1437, in: G. Milanesi (Ed.), Le Monnier Firenze, 1859.
[27] J. Molera, A. Climent-Font, T. Pradell, O. Vallcorba, A. Zucchiatti, Experimental study of historical processing of cobalt arsenide ore for colouring glazes (15 16th century Europe), J. Archeol. Sci.: Reports 36 (2021) 1–35, doi:10.1016/j.jasrep.2021.102797.
[28] G. Agricola, Bermannus Sive De *Re* Metallica Dialogus, Biblioteca Nazionale Braidense (1530) Milan.
[29] M. Smirniou, T. Rehren, Shades of blue e cobalt-copper coloured blue glass from New Kingdom Egypt and the Mycenaean world: a matter of production or colourant source? J. Archaeol. Sci. 40 (2013) 4731–4743, doi:10.1016/j.jas.2013.06.029.
[30] A.J. Shortland, H. Schroeder, Analysis of first millennium BC glass vessels and beads from the Pichvnari necropolis, Georgia, Archaeometry. 51 (6) (2009) 947–965, doi:10.1111/j.1475-4754.2008.00443.x.
[31] B. Gratuze, I. Pactat, N. Schibille, Changes in the Signature of Cobalt Colorants in Late Antique and Early Islamic Glass Production, Minerals 8 (2018) 225, doi:10.3390/min8060225.
[32] F. Fauth, I. Peral, C. Popescu, M. Knapp, The new material science powder diffraction beamline at ALBA Synchrotron, Powder. Diffr. 28 (2013) S360–S370, doi:10.1017/S0885715613000900.
[33] J.L. Campbell, T.L. Hopman, J.A. Maxwell, Z. Nejedly, The Gueplh PIXE package II: alternative proton database, Nucl. Instr. Meth. 170 (2000) 193–204 B.
[34] M. Matin, M. Pollard, From ore to pigment: a description of the minerals and an experimental study of cobalt ore processing from the Kāshān mine. Iran, Archaeometry. 59 (4) (2017) 731–746, doi:10.1111/arcm.12272.
[35] A.M. Isfahani, On the Manifacture of Modern Kashi Earthenware Tiles and Vases in Imitation of the ancient, Museum of Science and Art, Edinburgh, 1888.
[36] L.J. Olmer, Rapport Sur Une Mission Scientifique En Perse, Imprimerie Nationale, Paris, 1908.
[37] J. Rochechouart, Souvenirs D'un Voyage En Perse, Challamel, 1867.
[38] A.H. Schindler, Reisen im sudlichen Persien 1879, Zeitschriftder Gesellschaflfur ErdkundezuBerlin 16 (1881) 312–331 Eastern Persian Irak, J. Murray, London (1896).
[39] D. Krieg, Part of a letter from Dr David Krieg, F.R.S. to the publisher, concerning cobalt, and the preparations of smalt and arsenic. 'Philosoph. Trans.', vol. XXIV, n. 293 (1726 [ann. 1704-5]) 1754–1756.
[40] L. Bruzzone, Indagine Sperimentale Su Fasi Di Cobalto e Arsenico (eritrite e clinosafflorite) Nella Produzione Del Pigmento Blu Di Cobalto, University of Genova, 2023 Master ThesisUnpublished.
[41] M. Yu, C. Weidenthaler, Y. Wang, E. Budiyanto, E. Onur Sahin, M. Chen, S. DeBeer, O. Rüdiger, H. Tüysüz, Surface boron modulation on cobalt oxide nanocrystals for electrochemical oxygen evolution reaction, Angewandte Chemie Int. Ed. 61 (42) (2022) e202211543 1-12, doi:10.1002/anie.202211543.
[42] S.A. Mikhail, A.M. Turcotte, W.S. Bowman, A study of the decomposition of higher cobalt arsenides by thermal analysis, Thermochim. Acta 156 (1989) 287–296, doi:10.1016/0040-6031(89)85442-5.
[43] L.J. Wilson, S.A. Mikhail, Investigation of the oxidation of skutterudite by thermal analysis, Thermochim. Acta 156 (1989) 107–115, doi:10.1016/0040-6031(89)87176-X.